2010

Stresses In Reciprocating Compressor Discharge Tubes During Starting

James Robert Lenz
Tecumseh Products Company

Stresses in Reciprocating Compressor Discharge Tubes during Starting

James Lenz

[1]Tecumseh Products Company,
1136 Oak Valley Drive
Ann Arbor, MI, 48108
USA
Email: jim.lenz@tecumseh.com

ABSTRACT

A numerical method is presented for computing the time varying stresses in reciprocating compressor discharge tubes during starting. The tube is described using shell elements, and mounting springs are described using beam elements. Mass and stiffness matrices are assembled into a second order system of equations that is then solved in a time step fashion along with mechanism and induction motor equations

1. INTRODUCTION

1.1 The Purpose of Discharge Tubes

Hermetic compressors that use reciprocating pistons are commonly used in residential and commercial refrigeration. They are cheap, quiet and dependable. The pistons are typically driven by a crankshaft and connecting rod in a slider-crank mechanism. Due to the non-circular motion of the piston and connecting rod, it is impossible to balance the inertia forces in this type of compressor completely with counterweights. For this reason, hermetic reciprocating compressors mount the crankcase and motor on springs inside the housing and use a discharge tube, or shock loop, to pipe the compressed discharge gas out through the housing. This arrangement isolates the vibration of the moving parts from the outside world.

1.2 The Design of Discharge Tubes

The design of the discharge tube involves two competing concerns. On the one hand, the tube needs to be flexible enough to survive all motion the compressor might experience and at the same time it should minimize pressure drop. Pressure drop hurts efficiency. Increasing the length and decreasing the diameter of the tube makes it more flexible, but increases the pressure drop. Decreasing the length and increasing the diameter and may decrease the pressure drop, but could over-stress the material under some conditions. Thus, discharge tube design relies on two key analyzes, flow analysis and stress analysis. This paper discusses stress analysis.

1.3 Stresses in Discharge Tubes

Discharge tubes are stressed by two things, internal pressure and motion of the compressor. In this paper we will refer to the *compressor* as the internal assembly including the crankcase and all parts attached to it, like the motor, cylinder head, and all the moving parts. In hermetic compressors, this is the assembly internal to the outer shell (or housing.)

Discharge tube stresses due to internal pressure can be easily estimated using traditional pipe stresses formulas. More accurate stresses can be determined by applying pressure loads to a shell element model of the discharge tube.

Stresses due to motion of the compressor require a more rigorous analysis. The analyst needs to consider several types of motion. One significant way to stress a discharge tube is shipping motion. To determine these shipping stresses, a structural model is constructed using finite elements. The nodes at the housing end of the tube are completely constrained while nodes at the compressor end are all given the same prescribed displacement. As the motion of a compressor during shipping is not known, the analyst needs to make a number of assumptions about these prescribed displacements. Typically, the displacements are chosen as the maximum allowed by the internal

shipping stops. The individual X, Y, and Z-directions are each given their respective maximum allowable excursion values while constraining all other degrees of freedom at zero. A more extensive analysis might include various combinations of these conditions using both positive and negative displacements. When all cases are complete, the worst-case stress can be found. It should be noted that this analysis could be overly conservative because in reality, the compressor will rotate (about some axis in 3-dimensions) to relieve some of the elastic energy during these displacements.

Motion of the compressor during starting is another significant source of discharge tube stresses.

2. ANALYSIS

2.1 The Finite Element Model

Motion during starting of the compressor is found using a finite element model that includes shell elements for the discharge tube, beam elements for the springs, and a concentrated mass representing the compressor. The shell element model of the discharge tube is constrained completely at the housing end. We add rigid-link elements at the compressor end. These rigid-link elements connect nodes on the discharge tube to each other, to a node at the center of mass of the compressor, and to the nodes at the ends of the mounting springs. Originally, we planned to model the mounting springs by specifying a stiffness matrix for each spring. However in practice, it is difficult to find the full 6-by-6-stiffness matrix for a coil spring without first making a finite element model. So, the in our case, we simply added the beam element models for the coil springs to the discharge tube model and connect them all together with the appropriate rigid links. A typical model for a small residential compressor is shown in Figure 1.

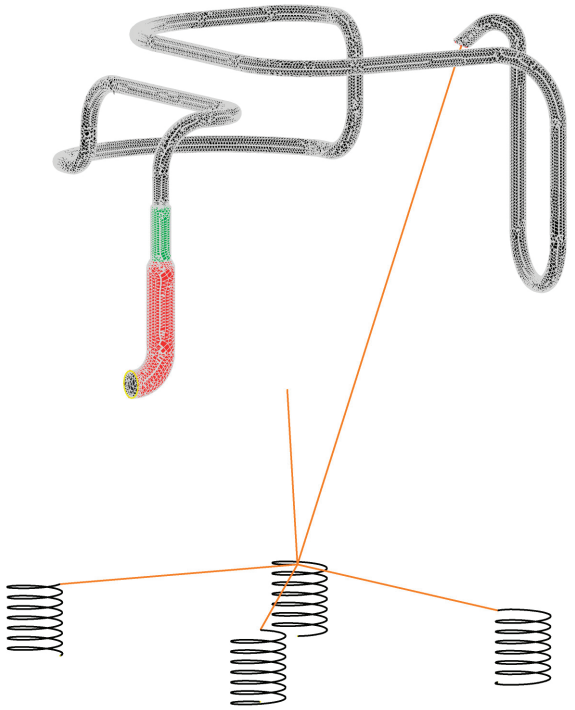

Figure 1: Finite element model of discharge tube with suspension system

Modeling the springs as a series of beam elements allows mass matrices to be constructed for these elements, making it possible to calculate natural frequencies and modes of the springs.

The discharge tube is modeled with 3-noded triangular flat shell elements. Zienkiewicz (1977) derived this element by assembling the plate-bending element of Bazeley, Cheung, Irons, and Zienkiewicz (1965) with a constant strain triangle. Each node of the shell element has the following degrees of freedom. Using T to denote vector transpose:

$$\mathbf{U}_{\text{node}} = \begin{bmatrix} u & v & w & \theta_x & \theta_y & \theta_z \end{bmatrix}^T \tag{1}$$

It should be noted that the plate-bending element of Bazeley, Cheung, Irons, and Zienkiewicz (1965) assumes down is positive. When using this element in a general-purpose shell element, a *(–w)* must first be substituted for *w*.

2.2 Equations of Motion

The assembled mass and stiffness matrices take the form of the following second order system of linear differential equations:

$$\mathbf{M}\ddot{\mathbf{U}} + \mathbf{C}\dot{\mathbf{U}} + \mathbf{K}\mathbf{U} = \mathbf{R} \tag{2}$$

where **M**, **C**, and **K** are the global mass, damping, and stiffness matrices; **R** is the global load vector; and $\mathbf{U}$, $\dot{\mathbf{U}}$, and $\ddot{\mathbf{U}}$ are the displacement, velocity and acceleration vectors of the system. Assuming Rayleigh damping (Bathe and Wilson. 1976), we obtain the damping matrix **C** as a linear combination of the mass and stiffness matrices.

$$\mathbf{C} = \xi\mathbf{M} + \beta\mathbf{K} \tag{3}$$

We take advantage of this relationship and compute the members of **C** as we need them and avoid storing the whole **C** matrix in memory. The weighting factors ξ and β can be estimated from knowledge of the modal damping ratios and how they vary with frequency.

2.3 Torque of an Induction Motor

The mathematical model of the start event involves adding a forcing term to **R** on the right-hand side of (2). Start with a free-body diagram that includes the compressor, discharge tube and mounting springs. Envision this by adding to Figure 1 the internal compressor assembly at the center-of-mass node. Solution of the system (2) will then satisfy the laws of motion if the following term is added to the correct entry in **R**.

$$R_{zi} = J\dot{\omega} \tag{4}$$

where R_{zi} is the entry in **R** for the z-rotation degree-of-freedom for node i, in this case, the center of mass node. *J* is the mass moment of inertia of the crankshaft and rotor and ω is the rotational speed of the crankshaft and rotor. Next, taking the crankshaft and rotor as a free body and assuming no cylinder pressure and further assuming that the mass of the piston and connecting rod are negligible we obtain the relation

$$J\dot{\omega} = T_m(\omega) \tag{5}$$

where T_m is the motor torque which is a function of rotor speed, ω, which in turn is a function of time. Motor torque as a function of speed can be adequately calculated using the an equation of the form given by Bukac (2002):

$$T_m = V^2 \cdot \frac{A_1 \cdot s}{B_2 \cdot s^2 + B_1 \cdot s + 1} \tag{6}$$

where *s* is the dimensionless slip given by

$$s = \frac{\omega_s - \omega}{\omega_s} \tag{7}$$

and the constants A_1, B_1 and B_2 are given by

$$A_1 = \frac{T_L \cdot T_M \cdot (2 \cdot s_M - s_M^2 - 1)}{V^2 \cdot s_M^2 \cdot (T_L - T_M)}; \qquad B_1 = \frac{2 \cdot T_M \cdot s_M - T_L \cdot (s_M^2 + 1)}{s_M^2 \cdot (T_L - T_M)}; \qquad B_2 = \frac{1}{s_M^2} \tag{8}$$

Equation (6) is substituted into equation (5) and solved as an initial-value problem for rotor speed, ω, as a function of time using a Second Order Runge-Kutta method (Conte and Boor,1972.) The torque is then computed from speed using (6).

2.4 Solution

The simulation involves using finite difference approximations to the time derivatives in system (2). The Newmark method uses the following finite difference approximations (Bathe and Wilson, 1976)

$$\ddot{\mathbf{U}}_{\mathbf{t+\Delta t}} = a_0(\mathbf{U}_{\mathbf{t+\Delta t}} - \mathbf{U}_{\mathbf{t}}) - a_2\dot{\mathbf{U}}_{\mathbf{t}} - a_3\ddot{\mathbf{U}}_{\mathbf{t}} \tag{9}$$

$$\dot{\mathbf{U}}_{\mathbf{t+\Delta t}} = \dot{\mathbf{U}}_{\mathbf{t}} + a_6\ddot{\mathbf{U}}_{\mathbf{t}} + a_7\ddot{\mathbf{U}}_{\mathbf{t+\Delta t}} \tag{10}$$

These are substituted into system (2) written for time t+Δt and solved for the unknown displacements $\mathbf{U_{t+\Delta t}}$. This results in the following system of linear of equations

$$\hat{\mathbf{K}}\mathbf{U}_{\mathbf{t+\Delta t}} = \hat{\mathbf{R}}_{\mathbf{t+\Delta t}} \tag{11}$$

where

$$\hat{\mathbf{K}} = \mathbf{K} + a_0\mathbf{M} + a_1\mathbf{C} \tag{12}$$

and

$$\hat{\mathbf{R}}_{\mathbf{t+\Delta t}} = \mathbf{R}_{\mathbf{t+\Delta t}} + \mathbf{M}(a_0\mathbf{U}_{\mathbf{t}} + a_2\dot{\mathbf{U}}_{\mathbf{t}} + a_3\ddot{\mathbf{U}}_{\mathbf{t}}) + \mathbf{C}(a_1\mathbf{U}_{\mathbf{t}} + a_4\dot{\mathbf{U}}_{\mathbf{t}} + a_5\ddot{\mathbf{U}}_{\mathbf{t}}) \tag{13}$$

and the constants a_0 through a_7 are defined as

$$\begin{gathered} a_0 = \frac{1}{\alpha\Delta t^2}; \quad a_1 = \frac{\delta}{\alpha\Delta t}; \quad a_2 = \frac{1}{\alpha\Delta t}; \quad a_3 = \frac{1}{2\alpha} - 1 \\ a_4 = \frac{\delta}{\alpha} - 1; \quad a_5 = \frac{\Delta t}{2}\left(\frac{\delta}{\alpha} - 2\right); \quad a_6 = \Delta t(1-\delta); \quad a_7 = \delta\Delta t \end{gathered} \tag{14}$$

Parameters α and δ can be varied to obtain optimum integration accuracy and stability. Newmark originally proposed as an unconditionally stable scheme the values

$$\alpha = \tfrac{1}{4}; \qquad \delta = \tfrac{1}{2}$$

At each time step, the torque computed in (6) is inserted into the forcing function vector $\mathbf{R_{t+\Delta t}}$ on right-hand side of (13) which is used in (11). System (11) is solved using a linear equation solver for $\mathbf{U_{t+\Delta t}}$.

3. RESULTS

Figure 2 shows the resulting motor torque as a function of time and Figure 3 shows crankshaft speed as a function of time for a typical refrigeration compressor. Peak torque is reached at about 0.04 seconds and final speed is reached shortly afterwards. The resulting rotation of the compressor about the z-axis is shown in Figure 4 and the stress at the location of peak stress is plotted as a function of time in Figure 5. The peak rotational displacement and the peak

stress are found to happen at 0.053 seconds. As can be seen, the peak stress happens very early in the process, almost certainly before any pressure has had a chance to build up on the high side of the system.

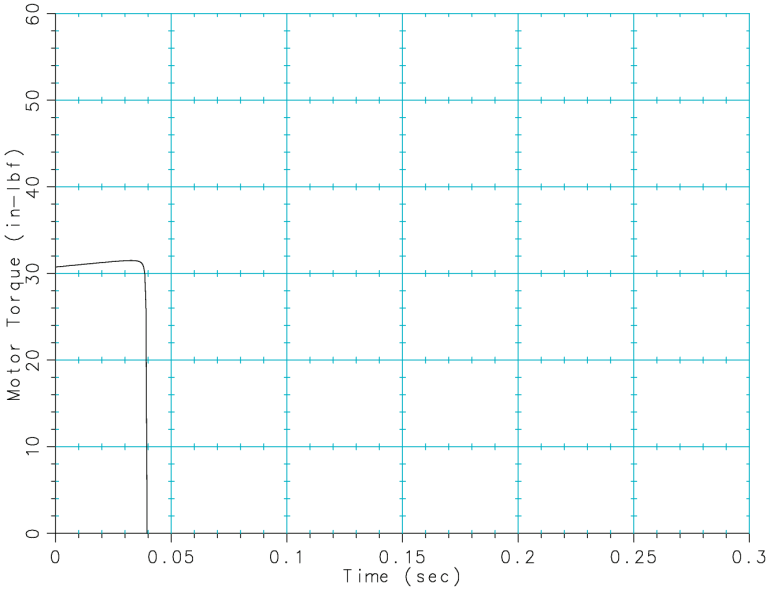

Figure 2: Motor torque as a function of time

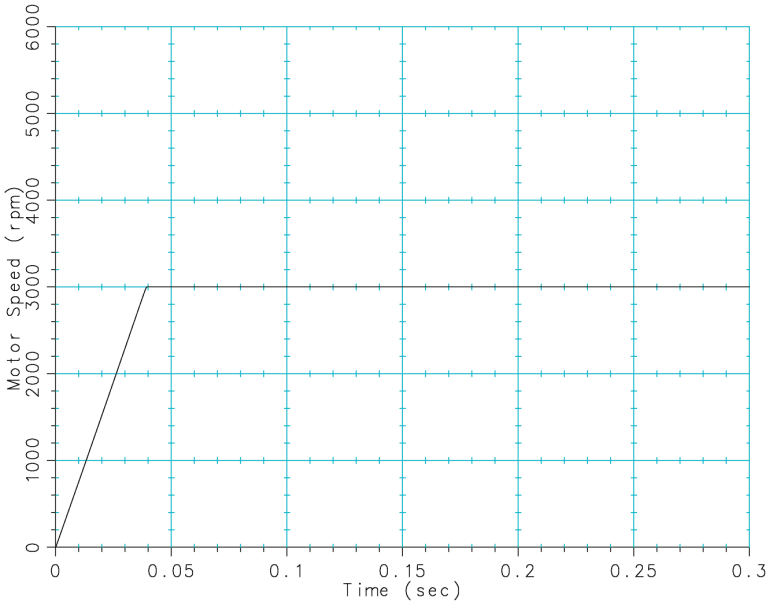

Figure 3: Crankshaft speed as a function of time

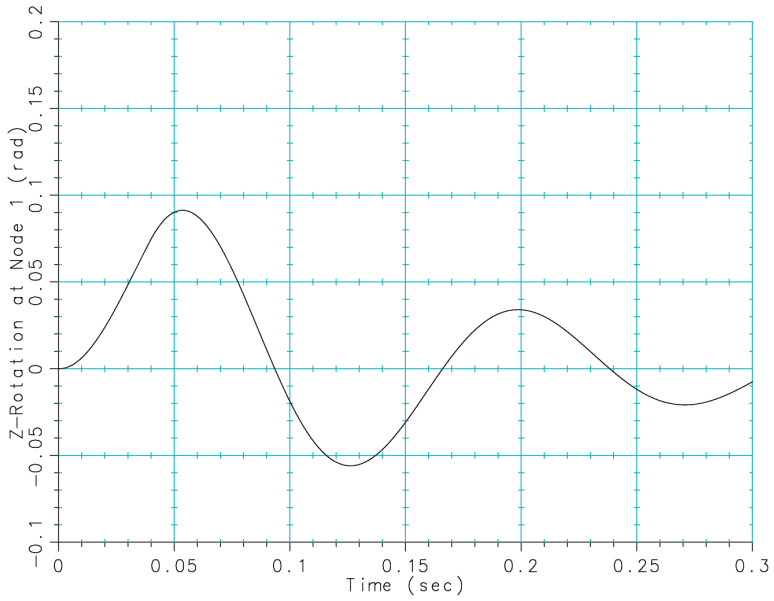

Figure 4: Crankcase rotation as a function of time

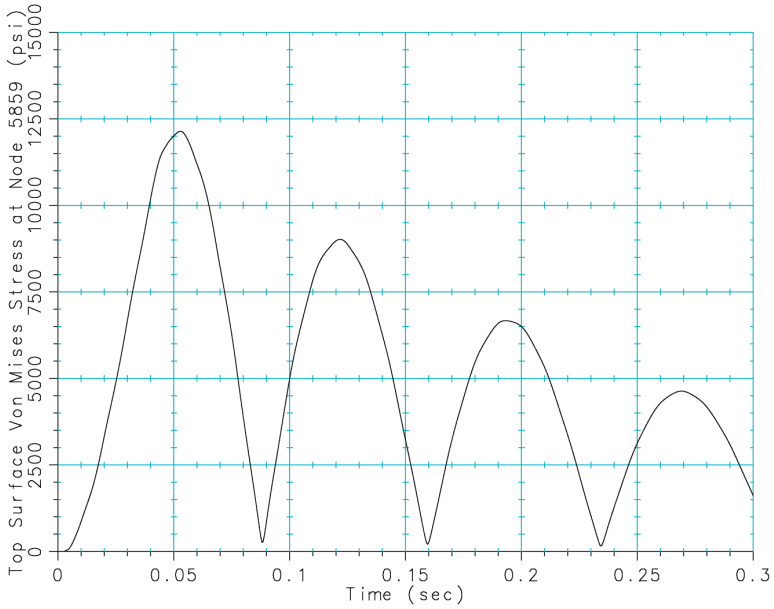

Figure 5: Discharge tube stress as a function of time

In general, the stress state at any given point is defined by 6 independent stresses, 3 normal stresses and 3 shear stresses. For the purposes of engineering calculations, these stresses are combined into a representative stress number that is appropriate to the failure mode for the particular problem. In our case, the failure mode is fatigue of a ductile material, so the representative stress is the Von Mises stress per Juvinall (1967). Certainly a more rigorous approach using individual stresses components in a fatigue damage calculation is possible using the finite element results. This will be investigated in future work.

Figure 6 shows a close-up view of the contours of Von Mises stress around the point of peak stress.

4. CONCLUSIONS

An analytical procedure has been presented that allows the calculation of stresses in discharge tubes during compressor start for a given tube geometry, suspension system design and motor curve.

Figure 6: Close-up view of Von Mises stresses at time=0.053 sec

NOMENCLATURE

α	First Newmark integration constant
β	Second Rayleigh damping constant
δ	Second Newmark integration constant
θ_x	Rotation about the x-axis, nodal
θ_y	Rotation about the y-axis, nodal
θ_z	Rotation about the z-axis, nodal
ξ	First Rayleigh damping constant
ω	Speed of rotation of crank & rotor
ω_s	Synchronous speed of motor
$\mathbf{C}$	Damping matrix, assembled global
J	moment of inertia crank & rotor about z
$\mathbf{K}$	Stiffness matrix, assembled global
$\hat{\mathbf{K}}$	Stiffness-like coefficient matrix in Newmark solver
$\mathbf{M}$	Mass matrix, assembled global
$\mathbf{R}$	Generalized force, assembled global
$\hat{\mathbf{R}}$	Force-like vector in Newmark solver
R_{zi}	Torque about z-axis at node i
t	Time at which solution is know
Δt	Time increment
t+Δt	Time at which solution is solved for
s	slip, dimensionless
s_M	slip at maximum torque
T_m	Torque of the motor
T_M	Maximum torque of the motor
T_L	Locked-rotor torque of the motor
u	Displacement in the x-direction, nodal
$\mathbf{U}$	Generalized displacement vector, global
$\mathbf{U_{node}}$	Generalized displacement vector, nodal
v	Displacement in the y direction, nodal
V	Motor Voltage
w	Displacement in the z direction, nodal
$\dot{\mathbf{U}}$	Derivative w.r.t. tme of displacement vector
$\ddot{\mathbf{U}}$	Second derivative w.r.t. time of displacement vector

REFERENCES

Bathe, K., Wilson, E., 1976, *Numerical Methods in Finite Element Analysis*, Prentice-Hall, Inc., Englewood Cliffs, p. 322-326, 339

Bazeley, G., Cheung, Y., Irons, B., Zienkiewicz, O., 1965, Triangular Elements in Bending – Conforming and Non-conforming Solutions, *Proc. Conf. Matrix Methods in Struct. Mech (October).,* Air Force Inst. Of Tech., Wright Patterson A.F. Base, Ohio

Bukac, H., 2002, Modeling Compressor Start Up, *Proc. of the Sixteenth International Compressor Engineering Conference at Purdue*, paper C12-6

Conte, S, de Boor, C, 1972, *Elementary Numerical Analysis, Second Edition*, McGraw-Hill, Inc., p. 336-338

Juvinall, R., 1967, *Engineering Considerations of Stress, Strain, and Strength*. McGraw-Hill, Inc., p. 86, 319

Zienkiewicz, O., 1977, The Finite Element Method, Third Edition, McGraw-Hill Book Company (UK) Limited, p. 329-355